



Experimental study on coupled caloric effect driven by dual fields in metamagnetic alloy ErCo₂[☆]

Liming Wu^{a, b, c}, Bingjie Wang^{c, d}, Fengxia Hu^{c, d, e, *}, Zhaojun Mo^{a, b, **,}, Houbo Zhou^{c, d}, Zhengying Tian^{c, d}, Yangyang Fan^c, Zhuo Yin^{c, d}, Zibing Yu^{c, d}, Jing Wang^{c, d}, Yunzhong Chen^c, Jirong Sun^{c, d}, Tongyun Zhao^{b, c}, Baogen Shen^{c, d, f, ***}

^a School of Rare Earths, University of Science and Technology of China, Hefei, 230026, China

^b Ganjiang Innovation Academy, Chinese Academy of Sciences, Ganzhou, 341119, China

^c Beijing National Laboratory for Condensed Matter Physics and State Key Laboratory of Magnetism, Institute of Physics, Chinese Academy of Sciences, Beijing, 100190, China

^d School of Physical Sciences, University of Chinese Academy of Sciences, Beijing, 101408, China

^e Songshan Lake Materials Laboratory, Dongguan, 523808, China

^f Ningbo Institute of Materials Technology and Engineering, Chinese Academy of Sciences, Ningbo, 315201, China

ARTICLE INFO

Article history:

Received 26 December 2023

Received in revised form

12 March 2024

Accepted 18 March 2024

Available online 20 March 2024

Keywords:

Rare earths

Magnetocaloric materials

Coupled caloric effect

Metamagnetic behavior

Dual fields

Magnetic-structure coupling

ABSTRACT

This study presents an experimental investigation of the coupled caloric effect driven by dual-fields in metamagnetic alloy ErCo₂ with strong magneto-structural coupling. Magnetic measurements were conducted under different pressures, revealing that the application of hydrostatic pressure stabilizes a small volume of paramagnetism (PM) phase, resulting in a shift of the phase transition temperature towards the low-temperature region. This shift is opposite to the temperature associated with the magnetic field-driven phase transition. As pressure increases, the metamagnetic transition in ErCo₂ is suppressed, and the hysteresis disappears. However, the produced cross-coupling caloric effect compensates the decrease in entropy change caused by the disappearance of the metamagnetic transition. As a result, a reversible giant magnetocaloric effect of 46.2 J/(kg·K) without hysteresis is achieved at a pressure of 0.910 GPa. Moreover, we propose that the temperature span of ErCo₂ can be significantly widened by optimizing the thermodynamic pathway of the magnetic and pressure fields, overcoming the defect of a narrow temperature range.

© 2024 Chinese Society of Rare Earths. Published by Elsevier B.V. All rights are reserved, including those for text and data mining, AI training, and similar technologies.

[☆] **Foundation item:** Project supported by the National Key R&D Program of China (2021YFB3501202, 2021YFB3501204, 2019YFA0704900, 2020YFA0711500, 2023YFA1406003, 2022YFB3505201), the National Natural Science Foundation of China (52088101, U23A20550, 92263202, 22361132534), and the Strategic Priority Research Program of the Chinese Academy of Sciences (XDB33030200).

* Corresponding author. Beijing National Laboratory for Condensed Matter Physics and State Key Laboratory of Magnetism, Institute of Physics, Chinese Academy of Sciences, Beijing, 100190, China.

** Corresponding author. School of Rare earths, University of Science and Technology of China, Hefei, 230026, China.

*** Corresponding author. Beijing National Laboratory for Condensed Matter Physics and State Key Laboratory of Magnetism, Institute of Physics, Chinese Academy of Sciences, Beijing, 100190, China.

E-mail addresses: fxhu@iphy.ac.cn (F. Hu), mozhaojun@gia.cas.cn (Z. Mo), shenbg@iphy.ac.cn (B. Shen).

<https://doi.org/10.1016/j.jre.2024.03.011>

1002-0721/© 2024 Chinese Society of Rare Earths. Published by Elsevier B.V. All rights are reserved, including those for text and data mining, AI training, and similar technologies.

1. Introduction

Solid-state refrigeration using the thermal effect of solids has attracted wide attention due to its high efficiency and extremely low greenhouse potential, and is poised to displace current refrigeration technologies that rely on the compression and expansion of environmentally harmful fluids. Solid-state thermal effects can be divided into magnetocaloric,^{1–3} elastocaloric⁴ and mechanocaloric effects.^{5–8} These effects correspond to the changes in magnetic ordering degree, electric dipole moment ordering degree, and lattice ordering degree, respectively, under external field influence. Additionally, the mechanical thermal effect can be classified into elastocaloric^{9–12} and barocaloric effect,^{6–8} based on the different methods of applying stress fields.

Since the initial report by Pecharsky and Gschneidner on the giant magnetocaloric effect in the first order phase transition

(FOPT) material $\text{Gd}_5\text{Si}_2\text{Ge}_2$ with magnetic-structure coupling,¹ extensive research has focused on the FOPT system involving magnetic-structure transition. Due to their magnetic-structural coupling phase transition properties, these materials typically demonstrate significant magnetocaloric effects and respond to both magnetic and mechanical fields. Examples of such materials include $\text{La}(\text{Fe},\text{Co},\text{Si})_{13}$ ^{13,14} and Ni-Mn based Heusler alloy^{8,15} systems. As a result, researchers have extensively studied the thermal effect of multi-field driving, or the multicaloric effect, during the recent years. Based on the ErCo_2 alloy, de Oliveira provided the first theoretical discussion that pressure and magnetic field can function as both driving and adjusting fields for the first-order magnetic-structure coupling phase transition materials.¹⁶ Further, researchers have theoretically explored the thermal effects of multi-field coupling through Landau phase transition theory^{17,18} and thermodynamic analysis.¹⁹ Compared to single-field driven thermal effects, the multicaloric effect boasts several advantages in: (1) expanding the temperature range of the phase transition and achieving the thermal effect at a wider temperature range¹⁹; (2) larger adjustment space with multi-field regulation, allowing lower fields to activate the phase transition²⁰; (3) increasing the entropy change of the phase transition process and improving the refrigeration efficiency.²¹

At the Curie temperature (T_C), ErCo_2 undergoes a FOPT with magnetic-structure coupling.^{22,23} The crystal structure changes from cubic (space group $Fd\bar{3}m$) to hexagonal (space group $R\bar{3}m$) simultaneously with a shift from paramagnetism (PM) to ferrimagnetism (FIM).^{22–24} Additionally, this transition causes a significant magnetocaloric effect.^{25,26} Meanwhile, as a model material for the study of the itinerant electron metamagnetism,^{27,28} ErCo_2 is particularly sensitive to external fields, especially pressure. While numerous studies have examined the effects of pressure on the magnetic properties and phase transition of ErCo_2 ,^{29,30} and have theoretically proposed that pressure and magnetic field can be used as driving fields to achieve higher magnetocaloric effect over a wider temperature range,¹⁶ however, the thermal effect caused by the coexistence of pressure and magnetic field is still not well understood and there is a lack of experimental research. In this paper, we report the coupled caloric effect driven by the magnetic field and hydrostatic pressure in the ErCo_2 alloy, which shows a first-order magnetic-structure coupling transition. The application of hydrostatic pressure stabilizes a small volume of PM phase, causing a shift of the phase transition temperature towards the low-temperature region, in the opposite direction to the magnetic field-driven phase transition temperature. The coupled caloric effect by magnetic and pressure field was analyzed using the thermodynamic theory of coupled caloric effect. With increasing pressure, the metamagnetic transition in ErCo_2 is suppressed and the hysteresis disappears. However, the reduction in thermal fluctuation resulting from the decrease of T_C and the contribution from cross-coupling thermal effect of magnetic field and pressure field ensures that the entropy change in the 0–5 T magnetic field does not decrease. A challenge in solid-state refrigeration is regulating the operating temperature while maintaining thermal effect strength. Based on the multicaloric effect contributed from coupled term, we propose that the temperature range of ErCo_2 can be widened significantly by combining magnetic field with pressure field, which provides a feasible strategy for solid-state phase change refrigeration.

2. Experimental

The ErCo_2 alloy with a nominal composition was fabricated using the arc-melting method in an argon atmosphere, incorporating a 3% excess of Er to compensate for volatilization. The

commercial purities of Er and Co are 99.9% and 99.97%, respectively. Homogenization was attained by remelting the ingots four times, subsequently sealed in quartz ampoules under an argon atmosphere, and annealed at 1273 K for 50 h, followed by quenching in liquid nitrogen. X-ray diffraction (XRD) was performed on powdered sample with $\text{Cu K}\alpha_1$ from 20° to 100° at the temperature of 5 and 300 K. Magnetic properties were measured using a superconducting quantum interferometer device (SQUID, MPMS-7 T). Hydrostatic pressure was applied by a Be–Cu pressure cell, with Daphne 7373 serving as the pressure transferring medium. The pressure inside the cell was calibrated using shifts in the superconductive transition temperature of Pb, which was placed alongside the specimen during measurements. Given the varied hysteresis effects exhibited by the specimen during the FOPT concerning temperature, magnetic field, and pressure, the testing procedure involved decreasing pressure, increasing temperature, and decreasing magnetic field. This approach aimed to mitigate potential inaccuracies in the measured results.

3. Results and discussion

The XRD patterns and Rietveld refinement of ErCo_2 compound at 5 and 300 K from 20° to 100° are shown in Fig. 1. The patterns indicate that the sample consists primarily of a single phase characterized by the MgCu_2 -type cubic Laves phase structure (space

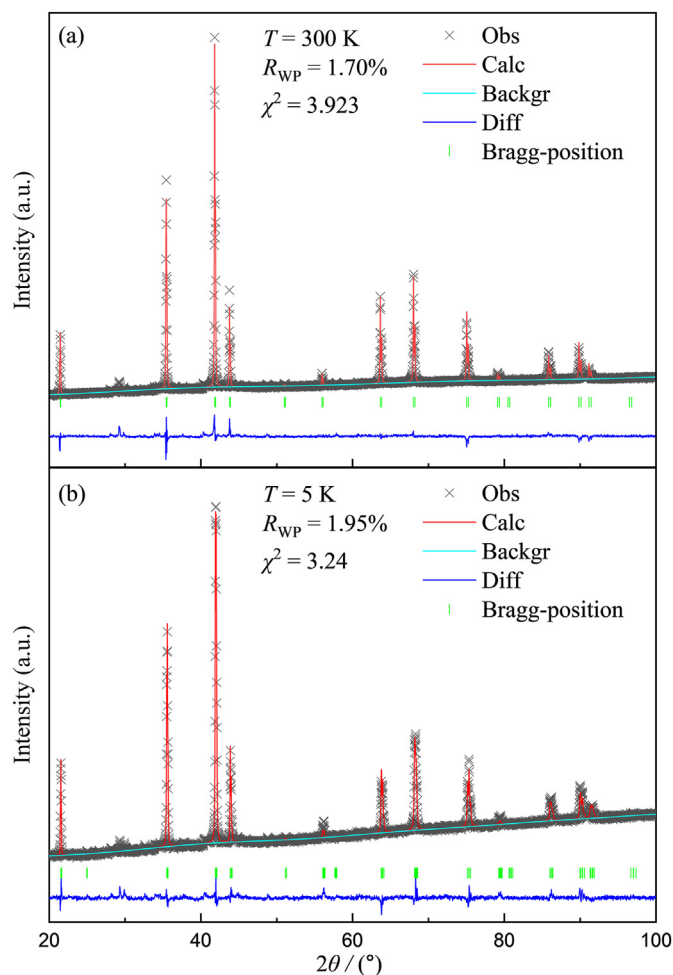


Fig. 1. XRD patterns of the ErCo_2 compound at 5 K (a) and 300 K (b) with corresponding Rietveld refinement.

group $Fd-3m$). While at 5 K, the crystal structure changes to rhombohedral structure (space group $R-3m$). Impurities are Er_2O_3 with several different structures and a total content of less than 3%. These rare earth oxides are antiferromagnetic at temperature of 3.4 K.³¹ As a result, there is no contribution to the magnetic behavior of the samples studied in the temperature range of interest.

Fig. 2(a) shows the curves of normalized magnetization versus temperature (M - T) for magnetic fields of 0.01, 1 and 5 T under ambient pressure. It is evident that the ErCo_2 sample undergoes a first-order magnetic phase transition (Fig. 2(b)), with the magnetic characteristics transforming from a PM state to a magnetically ordered state. Based on the temperature dependence of dM/dT as shown in the inset of Fig. 2(a), the Curie temperature, $T_C = 28$ K ($\mu_0H = 0.01$ T), increases with applied field at 1.42 K/T. This phenomenon is a result of the magnetic field stabilizing the FIM phase, which in turn increases the magnetic ordering temperature. Fig. 2(b) illustrates the normalized curves for the field-cooled (FC) and zero-field-cooled (ZFC) measurements taken at different hydrostatic pressures, ranging from 0 to 1.066 GPa (atmospheric pressure considered as 0 GPa), using a 0.01 T magnetic field. At various hydrostatic pressures, the FC curves experience sharp rise, which can be attributed to the magnetic phase transition from the FIM to the PM state, while the ZFC curves exhibit peaks, and the significant difference between the FC and ZFC magnetization curves originates from the domain wall pinning effect.³⁰ In the ZFC curves, domain walls are pinned at low temperatures, and the magnetization increases as the temperature increases, reaching a peak near T_C . However, in the FC curves, the magnetic field prevents the pinning of domain walls during cooling, resulting in the magnetization increase as the temperature decreases.³² In general, for materials undergoing negative thermal expansion, the pressure tends to stabilize the smaller phase, thus driving the phase transition temperature towards the low temperature region.^{33,34} Thus, at a magnetic field of 0.01 T, pressure drives the T_C of ErCo_2 at a rate of -5.6 K/T towards the lower temperatures, according to the inset of Fig. 2(b). This effect shows contrasts with the opposite impact of the magnetic field on the magnetic structure transition of ErCo_2 , which is also present in $\text{Fe}_{49}\text{Rh}_{51}$ ¹⁹ and $\text{Ni}_{50}\text{Mn}_{35}\text{In}_{15}$.³⁵

It is important to note that the itinerant electron metamagnetic transition caused by the transition group elements is responsible for the enormous magnetic entropy change in FOPT.^{36–38} Fig. 3(a) exhibits a metamagnetic transition nearby T_C in ErCo_2 ,

accompanied by a significant hysteresis as shown by the shaded area. Nonetheless, the metamagnetic transition in ErCo_2 progressively subsides at higher pressure. Fig. 3(b) illustrates the magnetization-field (M - H) curves at varying pressures and a temperature of 3 K above T_C . The S-shaped metamagnetic transition curve transforms into the magnetization curve of the PM phase through gradual transition as pressure increases. Furthermore, the magnetization and demagnetization curves gradually coincide, which means that the hysteresis disappears. For FOPT materials exhibit metamagnetic transitions, typically accompanied by hysteresis and resulting in irreversible changes in magnetic entropy. Common practice involves modulating the nature of the phase change through elemental substitution to eliminate the invariability of the magnetic transition. However, this approach often leads to a notable decrease in magnetic entropy change.^{39–41} Here, as pressure increases from 0 to 1.066 GPa, the peak of magnetic entropy change ($-\Delta S_M$) under 0–5 T magnetic field change remains almost constant. The difference is that the peak of $-\Delta S_M$ shifted by 6 K from 30 to 26 K towards the low-temperature region, as shown in Fig. 3(c). In addition to the positive contribution to the magnetic entropy change resulting from the reduction of thermal fluctuation due to the reduction of T_C ,⁴² the coupled caloric effect of pressure and magnetic field counterbalances the decrease in magnetic entropy change due to the vanishing of the metamagnetic transition.

Thermal effects in magneto-structurally coupled materials undergoing phase transitions driven by multiple fields can be analyzed simply from a thermodynamic perspective.¹⁹ Entropy, being a state function, remains independent of the order and path of the driving fields.²⁰ In a phase transition process driven by a magnetic field changing from 0 to μ_0H and a pressure change from 0 to p , the entropy change (ΔS) can be represented by the following path:

$$\Delta S[(0, 0) \rightarrow (p, \mu_0H)] = \Delta S[(0, 0) \rightarrow (p, 0)] + \Delta S[(p, 0) \rightarrow (p, \mu_0H)] \quad (1)$$

The first term on the right denotes the entropy change when altering the pressure from 0 to p while maintaining the external magnetic field at 0. This change is attributed to the barocaloric effect resulting from the applied pressure. In principle, the calculation of the barocaloric entropy change requires data on the pressure and temperature dependence of the specific volume. However, it can also be calculated from magnetization data as a function of temperature, pressure and magnetic field.¹⁹ The second

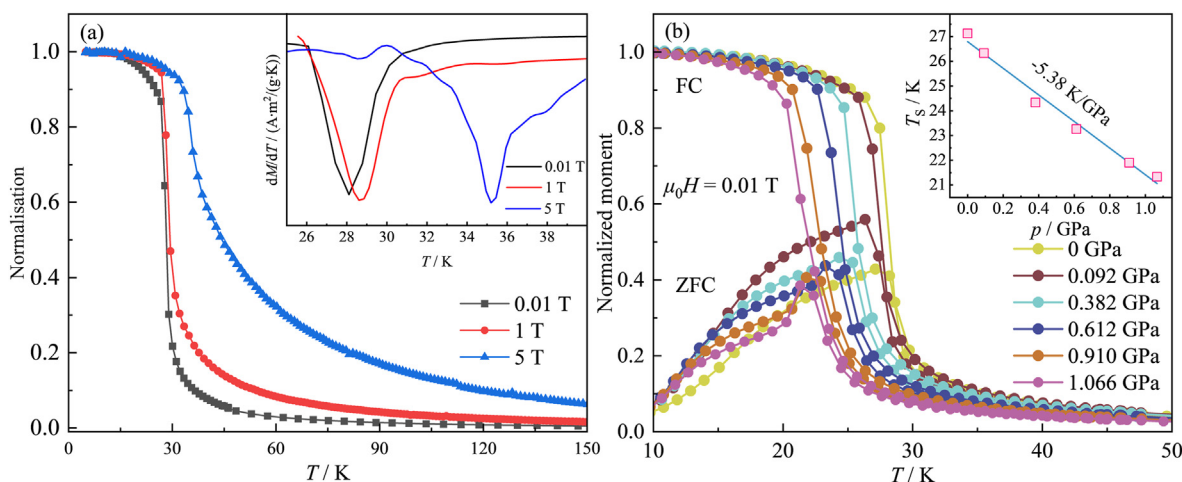


Fig. 2. (a) Normalized M - T curves for magnetic fields of 0.01, 1, and 5 T, and the inset shows dM/dT - T curves for the corresponding magnetic fields; (b) ZFC/FC curves ($\mu_0H = 0.01$ T) at 0, 0.092, 0.382, 0.612, 0.910 and 1.066 GPa, the inset shows the pressure dependence of T_C , which were calculated by dM/dT of FC curves.

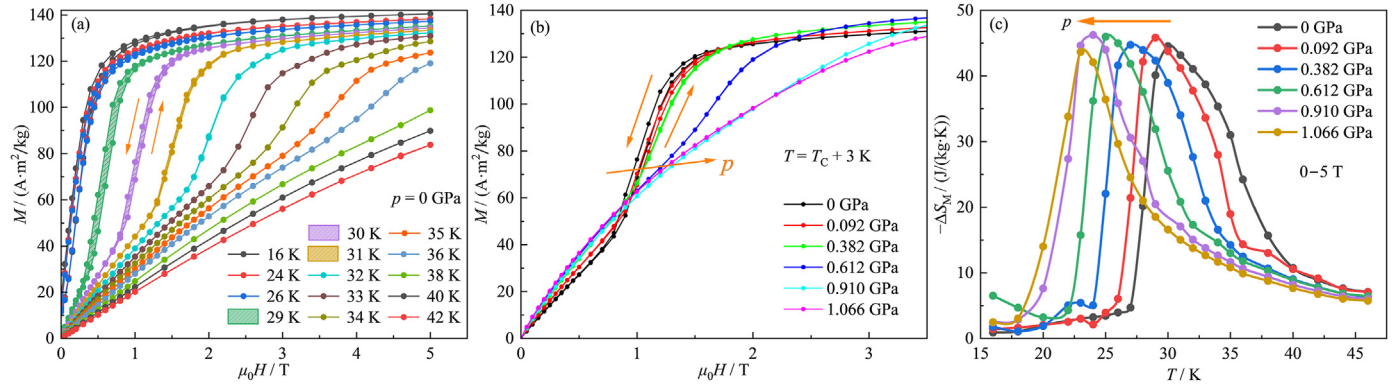


Fig. 3. Isothermal magnetization curves in ErCo₂ near T_C at 0 GPa (a) and above 3 K of T_C at pressure of 0, 0.092, 0.382, 0.612, 0.910 and 1.066 GPa (b) (the area shaded in (a) represents the hysteresis); (c) Entropy changes as a function of temperature calculated by Maxwell equation for a magnetic field range from 0 to 5 T at various pressures: 0, 0.092, 0.382, 0.612, 0.910 and 1.066 GPa.

term signifies the entropy change resulting from the alteration of the magnetic field from 0 to $\mu_0 H$ while keeping the pressure p constant. These two terms can be expressed as follows:

$$\Delta S[(0,0) \rightarrow (p, \mu_0 H)] = \int_0^p \left[\frac{\partial M}{\partial T} \right]_{p', \mu_0 H=0} dp' + \int_0^p \left[\frac{\partial M}{\partial T} \right]_{p, \mu_0 H'} d(\mu_0 H') \quad (2)$$

where M is the magnetization. The second term on the right-hand side of Eq. (2) can be expanded into the following two terms:

$$\int_0^p \left[\frac{\partial M}{\partial T} \right]_{p, \mu_0 H'} d(\mu_0 H') = \int_0^{\mu_0 H} \left[\frac{\partial M}{\partial T} \right]_{p, \mu_0 H'} d(\mu_0 H') + \int_0^p \int_0^{\mu_0 H} \frac{\partial \chi_{12}}{\partial T} dp' d(\mu_0 H') \quad (3)$$

According to Eqs. (1)–(3), the entropy change $\Delta S[(0,0) \rightarrow (p, \mu_0 H)]$ can be expressed as follows:

$$\Delta S[(0,0) \rightarrow (p, \mu_0 H)] = \int_0^p \left[\frac{\partial M}{\partial T} \right]_{p', \mu_0 H=0} dp' + \int_0^{\mu_0 H} \left[\frac{\partial M}{\partial T} \right]_{p, \mu_0 H'} d(\mu_0 H') + \int_0^p \int_0^{\mu_0 H} \frac{\partial \chi_{12}}{\partial T} dp' d(\mu_0 H') \quad (4)$$

The first term on the right-hand side of Eq. (4) represents the entropy change of the pressure-driven barocaloric effect (in the absence of a magnetic field); the second term represents the entropy change of the magnetic field-driven magnetocaloric effect (in the absence of a pressure); and the last term is the thermal effect of the cross-coupling term of the magnetic lattice, i.e., the coupling thermal effect, ΔS_{CP} :

$$\Delta S_{CP} = \int_0^p \int_0^{\mu_0 H} \frac{\partial \chi_{12}}{\partial T} dp' d(\mu_0 H') \quad (5)$$

where, χ_{12} is the cross-susceptibility that quantifies the response of p to the nonconjugated field $\mu_0 H$.

$$\chi_{12} = \left[\frac{\partial M}{\partial p} \right]_{T, \mu_0 H} \quad (6)$$

It indicates the strength of the interaction between ferroic properties, i.e., pressure and magnetic field. Therefore, due to the interaction between ferroic properties p and $\mu_0 H$, the multicaloric

effect is not a simple sum of the caloric effects associated with each one alone, but also includes the ΔS_{CP} .

Current research into the multicaloric effect concentrates on the effects of pressure on magnetocaloric or electrocaloric effects. Few studies have investigated the cross-coupled term of the magneto-mechanical or electro-mechanical coupled caloric effects. The multicaloric effect has been well understood theoretically through previous efforts.^{18,19,43} Experimentally, Enric et al.¹⁹ and Liang et al.³⁵ studied the magnetic field and pressure-driven cross-coupled term in Fe₄₉Rh₅₁ and Ni₅₀Mn₃₅In₁₅ alloys, respectively, providing detailed experimental analysis. For present ErCo₂, the M - p curves for the continuous phase transition region were derived by nonlinear numerical simulation utilizing experimentally measured magnetization data obtained at various pressures, as depicted in Fig. 4(a). Thereafter, the coupling term coefficient χ_{12} and coupled caloric effect ΔS_{CP} were calculated consecutively using Eqs. (6) and (5). The findings demonstrate that the thermal effect driven by the magnetic field at a certain pressure is the magnetocaloric effect under the ambient pressure regulated by the coupled caloric effect.^{19,35} That is to say:

$$\Delta S_{0 \text{ GPa}}[T, 0 \rightarrow \mu_0 H] + \int_0^p \int_0^{\mu_0 H} \frac{\partial \chi_{12}}{\partial T} dp' d(\mu_0 H') = \Delta S[T, p, 0 \rightarrow \mu_0 H] \quad (7)$$

Therefore, the ΔS_{CP} at different pressures was calculated using Eq. (7), based on analysis of the 5 T magnetic entropy change curves illustrated in Fig. 3(c) and presented in Fig. 4(b) for clarity. Fig. 4(c) further depicts a two-dimensional plot of Fig. 4(b). The coupling term gives rise to a negative peak with width and depth increasing gradually between 30 and 35 K, while simultaneously a positive peak emerges in the low temperature region. When the pressure reaches approximately 0.6 GPa, the negative peak steadily increases and shifts to lower temperatures. Although the rising tendency is weakened, there is no sign of saturation, even at a pressure of 1 GPa. Conversely, the positive peak progressively rises but saturates and moves towards lower temperatures. These behaviors reflect the evolution of the magnetic volume coupling coefficient χ_{12} with pressure and temperature. Absence of applied pressure results in χ_{12} and $-\Delta S_{CP}[T, p, 0 \rightarrow 5 \text{ T}]$ being 0 at 0 GPa. As pressure increases, $-\Delta S$ shifts towards the low-temperature region. The coupling term $-\Delta S_{CP}$ creates a negative peak close to $T_C = 35 \text{ K}$ to counterbalance the entropy change at 0 GPa, leading to a minimal entropy change at 35 K. Conversely, $-\Delta S_{CP}$ generates a positive peak in the low-temperature area, and with increasing pressure, it moves towards lower temperatures, indicating the shift in T_C

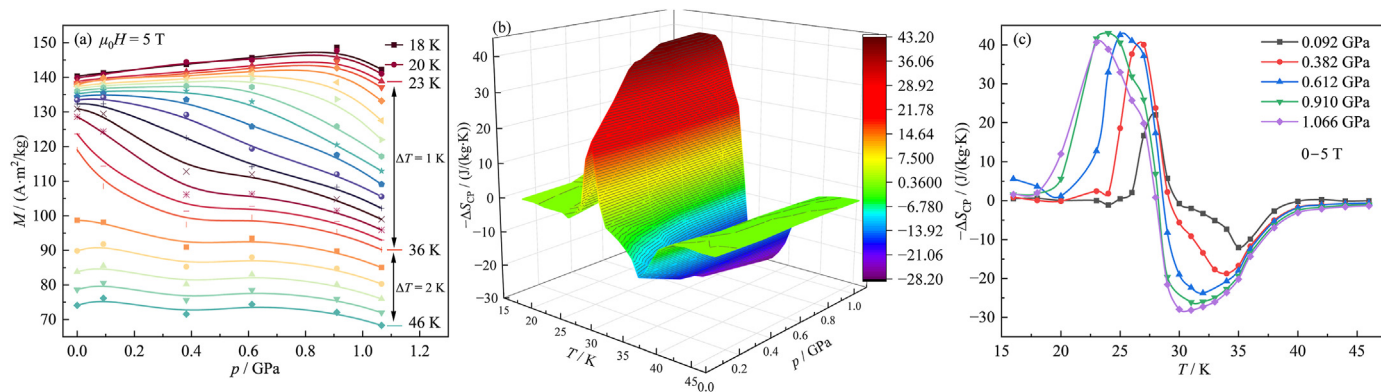


Fig. 4. (a) Magnetization as a function of pressure in the transition temperature region at a magnetic field of 5 T; Three-dimensional (b) and two-dimensional (c) plots of the $-\Delta S_{CP}[T, p, 0 \rightarrow 5 \text{ T}]$ as a function of pressure and temperature under a magnetic field change of 0–5 T.

towards the low-temperature area. The coupling term continues to increase at pressures below 0.6 GPa to compensate for the loss of the magnetic entropy change due to the disappearance of the metamagnetic transition. However, the metamagnetic transition is mostly suppressed at pressures greater than 0.6 GPa, whereas the coupling term tends to saturate. Therefore, although the disappearance of the metamagnetic transition causes a significant decrease in the magnetic entropy change, the decrease in T_C leads to the reduction of thermal fluctuation and the contribution of the coupled caloric term to the entropy change can keep the entropy change constant with the increase of the pressure in a 5 T magnetic field.

While the magnetic field and hydrostatic pressure induce contrasting effects on the magnetic structure transition of ErCo_2 , selecting the appropriate thermodynamic routes can surmount the inherent constraints of the monocoloric effect and significantly broaden the range of the cooling operating temperature. Here, we propose that the cooling of ErCo_2 over a wider temperature range can be accomplished by a method in which the magnetic field and hydrostatic pressure are applied and removed in a sequential manner, as indicated by the solid line 1 in Fig. 5. We begin at a high temperature under ambient pressure conditions and vary the

magnetic field from 0 to 5 T. Gradually, we decrease the temperature while retain the constant ambient pressure and magnetic field variation of 0 to 5 T until reaching the magnetic ordering temperature at 30 K. In the temperature range between 30 and 23 K, we maintain the same magnetic field variation and linearly increase the applied pressure from 0 at 30 K to 0.910 GPa at 23 K. The pressure remains constant at 0.910 GPa at temperatures below 23 K, and the magnetic field is adjusted between 0 and 5 T. For the sake of comparison, Fig. 5 also illustrates the $-\Delta S_M$ values obtained under constant pressures (ambient pressure and $p = 0.910 \text{ GPa}$) and when the magnetic field is altered from 0 to 5 T (dashed curves 2 and 3, respectively). By contrast, path 1, which combines a changing magnetic field with a changing hydrostatic pressure, can achieve a wider refrigeration operating temperature range than paths 2 and 3, which are fixed pressures. This further highlights the enormous advantage of multicoloric effect over monocoloric effects.

Hydrostatic pressure can enhance the magnetocaloric performance and create a tunable refrigeration operating temperature region in ErCo_2 . However, due to its low ordering temperature (close to 30 K), ErCo_2 cannot be used for room-temperature (RT) magnetic refrigeration, but it may be used for gas liquefaction. The multicoloric refrigeration strategy, which combines pressure and magnetic field, is generally applicable for refrigeration materials with magneto-structural coupling.⁴⁴ The multicoloric effect has been reported in various RT magnetic refrigeration materials, including $\text{La}(\text{Fe},\text{Si})_{13}$ alloys,⁴⁵ FeRh alloys,¹⁹ and Ni-Mn based Heusler alloys.¹⁵ Therefore, this strategy can also be used for refrigeration materials near room temperature. Although magnetic field and pressure variations at high frequencies are still challenging as far as current experimental techniques are concerned, the multi-calorimetric cooling techniques at mild frequencies should be optimistic, noting the recent developments in caloric materials and devices, as well as the advent of multicoloric cooling schemes.⁴⁴

4. Conclusions

In summary, we investigated the coupled caloric effects of ErCo_2 under magnetic field and pressure by magnetic measurements under hydrostatic pressure. Our findings indicate that the magnetic and pressure fields exert opposite influences on the phase transition temperature. With the increase of pressure, T_C moves to lower temperature, and the positive peak of coupled term $-\Delta S_{CP}$ gradually increases and tends to saturate at about 0.6 GPa. On the other hand, pressure causes the vanishing of the metamagnetic transition in ErCo_2 , leading to a decrease in entropy change and

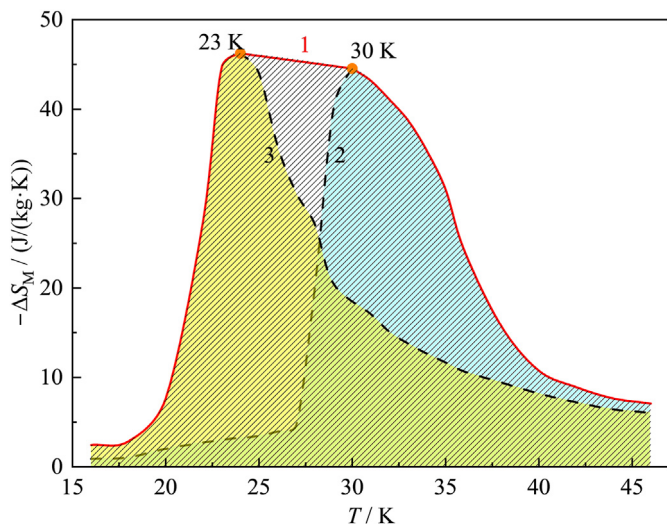


Fig. 5. Isothermal entropy change $-\Delta S_M$ for magnetic field from 0 to 5 T at 0 pressure and pressure linearly increasing from 0 GPa at 30 K to 0.910 GPa at 24 K (solid curve 1). Dashed lines indicate $-\Delta S_M$ for a magnetic field varying from 0 to 5 T at a fixed pressure $p = 0$ (dashed curve 2) and $-\Delta S_M$ for $p = 0.910 \text{ GPa}$ (dashed curve 3).

disappearance of hysteresis. However, the entropy change is partially compensated by $-\Delta S_{CP}$. As a result, a reversible giant magnetocaloric effect of 46.2 J/(kg·K) without hysteresis is achieved at a pressure of 0.910 GPa for magnetic field variations between 0 and 5 T. In addition to the extra coupled caloric effect, the magnetic field and pressure field can also widen the refrigeration temperature range by proper combination. This work proves that the multi-field driving can improve the calorics of first-order magnetic-structure coupled magnetocaloric materials, and solve the limitation of narrow working temperature range of FOPT refrigeration materials, providing a practical and feasible scheme for solid-state refrigeration applications.

Declaration of competing interest

The authors declare that they have no conflict of interest.

Acknowledgments

This work was also supported by the key programs of Chinese Academy of Sciences, China.

References

- Pecharsky VK, Gschneidner Jr KA. Giant magnetocaloric effect in $Gd_5(Si_2Ge_2)$. *Phys Rev Lett*. 1997;78(23):4494.
- Gong JJ, Fu Q, Sun H, Tian L, Gao X, Li Z, et al. Large reversible cryogenic magnetocaloric effect in rare earth iron carbides of composition RE_2FeC_4 (RE=Ho, Er, and Tm). *J. Rare Earths*. 2023;41(12):1996.
- Wei SJ, Shen HX, Zhang LY, Luo L, Tang XX, Sun JF, et al. Microstructure and magnetocaloric properties of melt-extracted $SmGdDyCoAl$ high-entropy amorphous microwires. *Rare Met*. 2024;43:1234.
- Peng BL, Fan HQ, Zhang Q. A giant electrocaloric effect in nanoscale antiferroelectric and ferroelectric phases coexisting in a relaxor $Pb_{0.8}Ba_{0.2}ZrO_3$ thin film at room temperature. *Adv Funct Mater*. 2013;23(23):2987.
- Bonnot E, Romero R, Manosa L, Vives E, Planes A. Elastocaloric effect associated with the martensitic transition in shape-memory alloys. *Phys Rev Lett*. 2008;100(12):125901.
- Ahadi A, Kawasaki T, Harjo S, Ko WS, Sun QP, Tsuchiya K. Reversible elastocaloric effect at ultra-low temperatures in nanocrystalline shape memory alloys. *Acta Mater*. 2019;165:109.
- Lu BF, Xiao F, Yan A, Liu J. Elastocaloric effect in a textured polycrystalline Ni-Mn-In-Co metamagnetic shape memory alloy. *Appl Phys Lett*. 2014;105(16):161905.
- Mañosa L, González-Alonso D, Planes A, Bonnot E, Barrio M, Tamarit JL, et al. Giant solid-state barocaloric effect in the Ni-Mn-In magnetic shape-memory alloy. *Nat Mater*. 2010;9(6):478.
- Cao YX, Zhou XL, Cong DY, Zhang HX, Cao YH, Nie ZH, et al. Large tunable elastocaloric effect in additively manufactured Ni-Ti shape memory alloys. *Acta Mater*. 2020;194:178.
- Cong DY, Xiong WX, Planes A, Ren Y, Mañosa L, Cao PY, et al. Colossal elastocaloric effect in ferroelastic Ni-Mn-Ti alloys. *Phys Rev Lett*. 2019;122(25):255703.
- Huang YJ, Hu QD, Bruno NM, Chen JH, Karaman I, Ross JH, et al. Giant elastocaloric effect in directionally solidified Ni-Mn-In magnetic shape memory alloy. *Scripta Mater*. 2015;105:42.
- Yang Z, Cong DY, Sun XM, Nie ZH, Wang YD. Enhanced cyclability of elastocaloric effect in boron-microalloyed Ni-Mn-In magnetic shape memory alloys. *Acta Mater*. 2017;127:33.
- Mañosa L, González-Alonso D, Planes A, Barrio M, Tamarit JL, Titov IS, et al. Inverse barocaloric effect in the giant magnetocaloric La-Fe-Si-Co compound. *Nat Commun*. 2011;2:595.
- Hu FX, Shen BG, Sun JR, Cheng ZH, Rao GH, Zhang XX. Influence of negative lattice expansion and metamagnetic transition on magnetic entropy change in the compound $LaFe_{11.4}Si_{1.6}$. *Appl Phys Lett*. 2001;78(23):3675.
- Qu YH, Cong DY, Li SH, Gui WY, Nie ZH, Zhang MH, et al. Simultaneously achieved large reversible elastocaloric and magnetocaloric effects and their coupling in a magnetic shape memory alloy. *Acta Mater*. 2018;151:41.
- de Oliveira NA. Entropy change upon magnetic field and pressure variations. *Appl Phys Lett*. 2007;90(5):052501.
- Meng H, Li B, Ren WJ, Zhang ZD. Coupled caloric effects in multiferroics. *Phys Lett*. 2013;377(7):567.
- Planes A, Castán T, Saxena A. Thermodynamics of multicaloric effects in multiferroics. *Philos Mag A*. 2014;94(17):1893.
- Stern-Taulats E, Castán T, Planes A, Lewis LH, Barua R, Pramanick S, et al. Giant multicaloric response of bulk $Fe_{49}Rh_{51}$. *Phys Rev B*. 2017;95(10):104424.
- Stern-Taulats E, Castán T, Mañosa L, Planes A, Mathur ND, Moya X. Multicaloric materials and effects. *MRS Bull*. 2018;43(4):295.
- Hao JZ, Hu FX, Zhou HB, Liang WH, Yu ZB, Shen FR, et al. Large enhancement of magnetocaloric effect driven by hydrostatic pressure in $HoCuSi$ compound. *Scripta Mater*. 2020;186:84.
- Gratz E, Markosyan AS. Physical properties of RCO_2 Laves phases. *J Phys Condens Matter*. 2001;13(23):385.
- Kozlenko DP, Burzo E, Vlaic P, Kichanov SE, Rutkauskas AV, Savenko BN. Sequential cobalt magnetization collapse in $ErCo_2$: beyond the limits of itinerant electron metamagnetism. *Sci Rep*. 2015;5:8620.
- Moon RM, Koehler WC, Farrell J. Magnetic structure of rare-earth-cobalt (RCO_2) intermetallic compounds. *J Appl Phys*. 1965;36(3):978.
- Herrero-Albillos J, Bartolomé F, García LM, Casanova F, Labarta A, Batlle X. Entropy change at the magneto structural transition in RCO_2 (R = Dy, Ho, Er). *J Magn Magn Mater*. 2006;301(2):378.
- Chen F, Xie H, Huo M, Wu H, Li L, Jiang Z. Effects of magnetic field and hydrostatic pressure on the antiferromagnetic–ferromagnetic transition and magneto-functional properties in $Hf_{1-x}Ta_xFe_2$ alloys. *Tungsten*. 2023;5(4):503.
- Duc NH, Goto T. Chapter 171 Itinerant electron metamagnetism of co sublattice in the lanthanide-cobalt intermetallics. In: Gschneidner Jr KA, Eyring L, eds. *Handbook on the physics and chemistry of rare earths*. Amsterdam: Elsevier; 1999.
- Herrero-Albillos J, Bartolomé F, García LM, Young AT, Funk T, Campo J, et al. Observation of a different magnetic disorder in $ErCo_2$. *Phys Rev B*. 2007;76(9):94409.
- Yamada H. Pressure effect in an itinerant-electron metamagnet at finite-temperature. *J Magn Magn Mater*. 1995;139(1–2):162.
- Singh NK, Kumar P, Suresh KG, Nigam AK, Coelho AA, Gama S. Measurement of pressure effects on the magnetic and the magnetocaloric properties of the intermetallic compounds $DyCo_2$ and $Er(Co_{1-x}Si_x)_2$. *J Phys Condens Matter*. 2007;19(3):036213.
- Moon RM, Koehler WC, Child HR, Raubenheimer LJ. Magnetic structures of Er_2O_3 and Yb_2O_3 . *Phys Rev*. 1968;176(2):722.
- Singh NK, Suresh KG, Nigam AK. Itinerant electron metamagnetism and magnetocaloric effect in $Dy(Co,Si)_2$. *Solid State Commun*. 2003;127(5):373.
- Hao JZ, Hu FX, Wang JT, Shen FR, Yu ZB, Zhou HB, et al. Large enhancement of magnetocaloric and barocaloric effects by hydrostatic pressure in $La(Fe_{0.92}Co_{0.08})_{11.9}Si_{1.1}$ with a $NaZn_{13}$ -type structure. *Chem Mater*. 2020;32(5):1807.
- Yibole H, Pathak AK, Mudryk Y, Guillou F, Zarkevich N, Gupta S, et al. Manipulating the stability of crystallographic and magnetic sub-lattices: a first-order magnetoelastic transformation in transition metal based Laves phase. *Acta Mater*. 2018;154:365.
- Liang FX, Hao JZ, Shen FR, Zhou HB, Wang J, Hu FX, et al. Experimental study on coupled caloric effect driven by dual fields in metamagnetic Heusler alloy $Ni_{50}Mn_{35}In_{15}$. *Appl Mater*. 2019;7(5):365.
- Tegus O, Bruck E, Zhang L, Dagula Buschow KHJ, de Boer FR. Magnetic-phase transitions and magnetocaloric effects. *Phys B Condens Matter*. 2002;319(1–4):174.
- Wang DH, Tang SL, Huang SL, Su ZH, Han ZD, Du YW. The origin of the large magnetocaloric effect in RCO_2 (R = Er, Ho and Dy). *J Alloys Compd*. 2003;360(1–2):11.
- Yamada H, Goto T. Itinerant-electron metamagnetism and giant magnetocaloric effect. *Phys Rev B*. 2003;68(18):184417.
- Lu GY, Du YS, Wu XF, Ma L, Li L, Cheng G, et al. Effect of Cu substitution on the type of magnetic phase transition and magnetocaloric effect in the $ErCo_{2-x}Cu_x$ compounds. *J Alloys Compd*. 2022;906:164343.
- Wada H, Tanabe Y, Shiga M, Sugawara H, Sato H. Magnetocaloric effects of Laves phase $Er(Co_{1-x}Ni_x)_2$ compounds. *J Alloys Compd*. 2001;316(1–2):245.
- Singh NK, Tripathy SK, Banerjee D, Tomy CV, Suresh KG, Nigam AK. Effect of Si substitution on the magnetic and magnetocaloric properties of $ErCo_2$. *J Appl Phys*. 2004;95(11):6678.
- Singh NK, Suresh KG, Nigam AK, Malik SK, Coelho AA, Gama S. Itinerant electron metamagnetism and magnetocaloric effect in RCO_2 -based Laves phase compounds. *J Magn Magn Mater*. 2007;317(1–2):68.
- Planes A, Castán T, Saxena A. Thermodynamics of multicaloric effects in multiferroic materials: application to metamagnetic shape-memory alloys and ferrotoroidics. *Philos Trans Royal Soc A*. 2016;374(2074):20150304.
- Gottschall T, Gràcia-Condal A, Fries M, Taubel A, Pfeuffer L, Mañosa L, et al. A multicaloric cooling cycle that exploits thermal hysteresis. *Nat Mater*. 2018;17(10):929.
- Hao JZ, Hu FX, Wang JT, Shen FR, Yu ZB, Zhou HB, et al. Large enhancement of magnetocaloric and barocaloric effects by hydrostatic pressure in $La(Fe_{0.92}Co_{0.08})_{11.9}Si_{1.1}$ with a $NaZn_{13}$ -type structure. *Chem Mater*. 2020;32(5):1807.